

Nuclear Stopping in Au+Au Collisions at $P_{\text{NN}} = 200 \text{ GeV}$

I. G. Bearden⁷, D. Beavis¹, C. Besliu¹⁰, B. Budick⁶, H. B. ggild⁷, C. Chasm an¹, C. H. Christensen⁷, P. Christiansen⁷, J. Cibor³, R. D ebbe¹, E. Enger¹², J. J. Gaardh je⁷, M. Germ inario⁷, K. H agef⁸, O. Hansen⁷, A. Holm⁷, A. K. Holm e¹², H. Ito^{11;1}, A. Jipa¹⁰, F. Jundt², J. I. J rdre⁹, C. E. J rgensen⁷, R. K arabow icz⁴, E. J. K im^{1;11}, T. K ozik⁴, T. M. Larsen¹², J. H. Lee¹, Y. K. Lee⁵, G. L. vh iden¹², Z. M. a jka⁴, A. M akiev⁸, M. M ikelsen¹², M. M urray^{8;11}, J. N atow itz⁸, B. S. N ielsen⁷, J. N orris¹¹, K. O lchanski¹, D. O uerdane⁷, R. P laneta⁴, F. R am f, C. R istea¹⁰, D. R ohrich⁹, B. H. Sam set¹², D. Sandberg⁷, S. J. Sanders¹¹, R. A. Scheetz¹, P. Staszek^{7;4}, T. S. T veter¹², F. V ideb k¹, R. W ada⁸, Z. Y in⁹, I. S. Zgura¹⁰

The BRAHMS Collaboration

¹ Brookhaven National Laboratory, Upton, New York 11973

² Institut de Recherches Subatomiques and Universite Louis Pasteur, Strasbourg, France

³ Institute of Nuclear Physics, Krakow, Poland

⁴ Smoluchowski Inst. of Physics, Jagiellonian University, Krakow, Poland

⁵ Johns Hopkins University, Baltimore 21218

⁶ New York University, New York 10003

⁷ Niels Bohr Institute, Blegdamsvej 17, University of Copenhagen, Copenhagen 2100, Denmark

⁸ Texas A & M University, College Station, Texas, 17843

⁹ University of Bergen, Department of Physics, Bergen, Norway

¹⁰ University of Bucharest, Romania

¹¹ University of Kansas, Lawrence, Kansas 66045

¹² University of Oslo, Department of Physics, Oslo, Norway

(Dated: Version: stopping.tex, December 31, 2003)

Transverse momentum spectra and rapidity densities, dN/dy , of protons, antiprotons, and net protons ($p - p$) from central (0-5%) Au+Au collisions at $P_{\text{NN}} = 200 \text{ GeV}$ were measured with the BRAHMS experiment within the rapidity range $0 \leq y \leq 3$. The proton and antiproton dN/dy decrease from mid-rapidity to $y = 3$. The net proton yield is roughly constant for $y < 1$ at $dN/dy \approx 7$, and increases to $dN/dy \approx 12$ at $y = 3$. The data show that collisions at this energy exhibit a high degree of transparency and that the linear scaling of rapidity loss with rapidity observed at lower energies is broken. The energy loss per participant nucleon is estimated to be $72 \pm 6 \text{ GeV}$.

PACS numbers: 25.75 Dw.

The energy loss of colliding nuclei is a fundamental quantity determining the energy available for particle production (excitation) in heavy ion collisions. This deposited energy is essential for the possible formation of a deconfined quark-gluon phase of matter (QGP). Because baryon number is conserved, and rapidity distributions are only slightly affected by rescattering in late stages of the collision, the measured net-baryon ($B - \bar{B}$) distribution retains information about the energy loss and allows the degree of nuclear stopping to be determined. Such measurements can also distinguish between different proposed phenomenological mechanisms of initial coherent multiple interactions and baryon transport [1, 2, 3].

The average rapidity loss, $h_{\text{yi}} = y_p - h_{\text{yi}}$ [21], is used to quantify stopping in heavy ion collisions [4, 5]. Here, y_p is rapidity of the incoming projectile and h_{yi} is the mean net-baryon rapidity after the collision:

$$h_{\text{yi}} = \frac{2}{N_{\text{part}}} \int_0^{y_p} y \frac{dN_{(B - \bar{B})}(y)}{dy} dy; \quad (1)$$

where N_{part} is the number of participating nucleons in the collision. The two extremes correspond to full stopping, where initial baryons lose all kinetic energy ($h_{\text{yi}} = y_p$) and full transparency, where they lose no kinetic energy ($h_{\text{yi}} = 0$). For fixed collision geometry (system size and centrality) at lower energy (SIS, AGS, and SPS) it was observed that h_{yi} is proportional to the projectile rapidity. For central collisions between heavy nuclei (Pb, Au), $h_{\text{yi}} \approx 0.58 \pm 0.05$ [5, 6, 7].

Bjorken assumed that sufficiently high energy collisions are "transparent", thus the mid-rapidity region is approximately net-baryon free [8]. The energy density early in the collision, ϵ , can then be related in a simple way to the final particle production. At RHIC it has been estimated that $\epsilon \approx 5 \text{ GeV/fm}^3$, well above the lattice QCD prediction ($\epsilon_{\text{crit}} \approx 1 \text{ GeV/fm}^3$ [9]) for the hadron gas to QGP phase transition.

In this letter, results on proton and antiproton production, and baryon stopping in Au+Au collisions at $P_{\text{NN}} = 200 \text{ GeV}$ are presented. The data were collected with the BRAHMS detector at RHIC.

The BRAHMS experiment consists of two independent spectrometer arms, the Mid-Rapidity Spectrometer (MRS) and the Forward Spectrometer (FS), described in detail in [10]. The spectrometers consist of dipole magnets, Time Projection Chambers (TPC) and Drift Chambers (DC) for tracking charged particles, and detectors for particle identification (PID). The MRS can be rotated $30^\circ < \theta < 95^\circ$ and the FS $23^\circ < \theta < 30^\circ$, where θ is the polar angle with respect to the beam axis. By combining different settings of angle and magnetic fields, (anti-)proton transverse momentum spectra at different rapidities ($0 < y < 3$) were obtained.

The interaction point (IP) is determined by the Beam-Beam counters (BB), with a precision of $\sigma_{BB} = 0.7$ cm. The IP was required to be within 15 (20) cm of the nominal IP for the MRS (FS) analysis to minimize acceptance corrections.

Protons and anti-protons are identified using Time-Of-Flight (TOF) light detectors (TOFW) in the MRS (TOFW) and FS (H1 and H2), and by the Ring Imaging Cherenkov (RICH) in the FS. The TOF resolution is $\sigma_{TOFW} = 80$ ps, $\sigma_{H1} = \sigma_{H2} = 90$ ps. To identify (anti-)protons it is required that the derived square of the mass, m^2 , is within 2% of the proton m^2 and at least 2% away from the m^2 for kaons. This allows (anti-)protons to be identified up to momentum $p < 3.0$ GeV/c for TOFW, $p < 4.5$ GeV/c for H1, and $p < 6.5$ GeV/c for H2. The low refractive index of the RICH, $n = 1.0020$ allows protons to be directly identified via a measurement of their ring radius in the range $15 < p < 25$ GeV/c. By using the RICH to veto pions and kaons the PID can be extended down to $p = 10$ GeV/c.

The collision centrality is determined using a multiplicity array located around the nominal IP [10]. In this analysis only the 0-5% most central collisions were used. The number of participants for this centrality class was found by Glauber model calculations to be $N_{part} = 357 \pm 8$ [11].

From the identified particles, invariant differential yields $\frac{1}{2} \frac{d^2N}{p_T dy dp_T}$ were constructed for each spectrometer setting. The differential yields were corrected for geometrical acceptance, tracking and PID efficiency, absorption and multiple scattering. The corrections for absorption and multiple scattering were less than 20% at the lowest p_T and less than 5% at the highest p_T in all settings. No corrections were applied for secondary protons from e.g. the beam pipe, since the contribution was found to be negligible in GEANT based Monte Carlo (MC) simulations [12] using HIJING [13] as input, when the tracks were required to point back to the IP. The acceptance correction is purely geometrical and calculated using a MC simulation of the BRAHMS detector. The tracking efficiency was estimated for the TPCs, by embedding simulated tracks in real events (method I), and in the

FS where there are 5 tracking detectors (2 TPCs and 3 DCs) by comparing the number of identified track segments in the chamber to the number of reference tracks determined by other detectors disregarding the chamber under consideration (method II). In the front part of the FS (FFS) where both methods are applicable, there was a 10% discrepancy between the two methods which has been included in the systematic errors quoted below. For the spectrometers the total tracking efficiency depends on the spectrometer angle and is 90-95% in the MRS, 80-90% in the FFS (settings at $y = 2$) and 60-70% in the full FS ($y = 2$, $y = 3$). The efficiencies of the TOF detectors were found to be 93-98%. For the part of the spectrum at $y = 3$, where the RICH was used to veto pions and kaons a correction for contamination of pions and kaons with no identified ring radius was applied. The RICH efficiency is 5%.

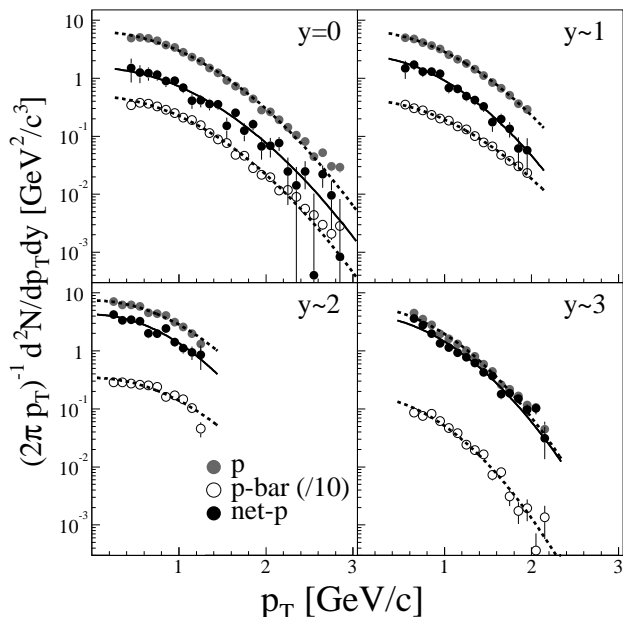


FIG. 1: Proton, anti-proton, and net-proton transverse momentum spectra at selected rapidities, $y = 0; 1; 2; 3$. The solid and dashed lines represent Gaussian fits to the data (extended outside the fit range for clarity). The anti-proton spectra have been divided by 10 as indicated. The error on the data points are statistical only and no weak decay correction has been applied.

Figure 1 shows transverse momentum spectra for four of the nine measured rapidities. The net-proton spectra were constructed by subtracting the anti-proton spectrum from the proton spectrum. At each rapidity, the proton, anti-proton, and net-proton spectra have similar shape, indicating that produced and transported protons have similar spectral properties. To obtain rapidity densities, dN/dy , for $p; p$ and net-p their spectra are fitted, and the fit was used to

extrapolate to the full p_T range. Different functional forms were tested: m_T -exponential, Boltzmann and Gaussian. The function found to best describe the data was the Gaussian in p_T [$f(p_T) / e^{p_T^2/(2^2)}$] and this function has been used for all fits.

The mean transverse momentum h_{p_T} of the spectra calculated from the fits is found to be within 0.1 GeV/c at each rapidity for the three spectra. For protons which have the best counting statistics, h_{p_T} decreases from $h_{p_T} = 1.01 \pm 0.01$ (stat) GeV/c at $y = 0$ to $h_{p_T} = 0.84 \pm 0.01$ (stat) GeV/c at $y = 3$.

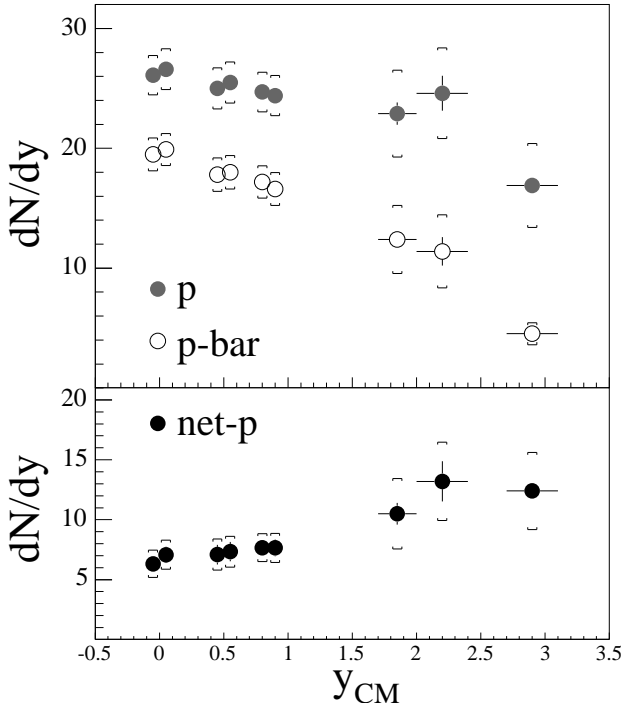


FIG. 2: Proton, anti{proton, and net{proton rapidity densities dN/dy as a function of rapidity at $\sqrt{s_{NN}} = 200$ GeV. The horizontal bars show the rapidity intervals for the projections. The errors shown with vertical lines are statistical only while the caps includes both statistical and systematic. No weak decay correction has been applied.

The differential yield within the measured p_T range varies from 85% of the total dN/dy near mid{rapidity to 45% at $y = 3$. The systematic errors on dN/dy were estimated from the difference in dN/dy values obtained using different spectrometer settings covering the same ($y; p_T$) regions, the discrepancy between the two different efficiency methods, and by estimating the effects of the p_T extrapolation. The systematic errors were found to be 10-15% for mid-rapidity ($y < 1$) and 20-30% for forward rapidities.

Figure 2 shows the resulting rapidity densities dN/dy as a function of rapidity. The most prominent feature of the data is that while the proton and anti{proton dN/dy decrease at rapidities away from mid{rapidity the net{proton dN/dy increases over all three

units of rapidity, from $dN/dy(y=0) = 6.4 \pm 0.4$ (stat) ± 1.0 (syst) to $dN/dy(y=3) = 12.4 \pm 0.3$ (stat) ± 3.2 (syst).

A Gaussian fit to the antiproton dN/dy distribution gives the total extrapolated anti{proton yield : 84.6 (92% in $3 < y < 3$). For protons the yield from a Gaussian fit to dN/dy in the range, $3 < y < 3$, is 138.7.

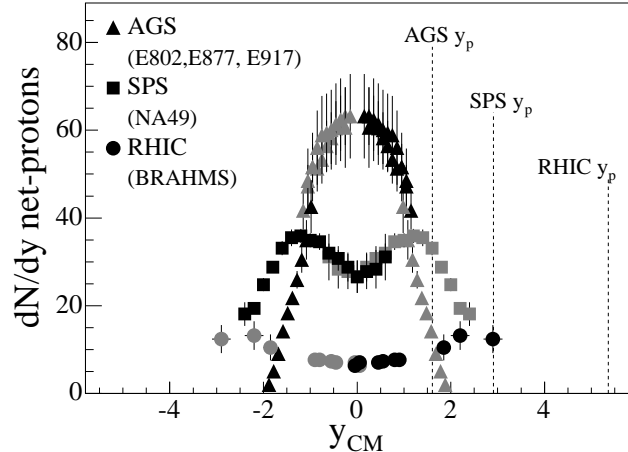


FIG. 3: The net{proton rapidity distribution at AGS [7, 14, 15], SPS [16] ($\sqrt{s_{NN}} = 5$ GeV), and this measurement ($\sqrt{s_{NN}} = 200$ GeV). The data are all from the top 5% most central collisions and the errors are both statistical and systematic. The data have been symmetrized. For RHIC data black points are measured and grey points are symmetrized, while the opposite is true for AGS and SPS data (for clarity). At AGS weak decay corrections are negligible and at SPS they have been applied.

Figure 3 shows net{proton dN/dy measured at AGS and SPS compared to these results. The distributions show a strong energy dependence, the net{protons peak at mid{rapidity at AGS, while at SPS a dip is observed in the middle of the distribution. At RHIC a broad minimum has developed spanning several units of rapidity, indicating that at RHIC energies collisions are quite transparent.

To calculate the rapidity loss, dN/dy must be known from mid{rapidity to projectile rapidity, $y_p = 5.36$. BRAHMS measures to $y = 3$, so the shape of the rapidity distribution must be extrapolated to calculate h_{yi} . The baryon number of participating nucleons (N_{part}) is conserved, while the net{proton number is not necessarily conserved. To obtain net{baryons, the number of net{neutrons and net{hyperons have to be estimated and the contribution from weak decays included in the measured net{protons has to be deduced. Using MC simulations we find this contribution (c) to be $c = 0.53 \pm 0.05$ protons for each decay. There is a weak rapidity dependence which is included in the systematic error. The number of net{baryons

is, then,

$$\begin{aligned} N_{B-B} &= (N_{p-p} - cN) \left(1 + \frac{N_n}{N_p}\right) + N \\ &= N_{p-p} \left(1 + \frac{N_n}{N_p}\right) + (1 - c(1 + \frac{N_n}{N_p}))N; \end{aligned} \quad (2)$$

where N_{p-p} is the measured net(proton yield, and $N_n; N_p$ and N are the primary number of net-neutrons, net-protons, and net-baryons, respectively. In addition to primaries, net-baryons, N includes contributions from other hyperons that decay to protons through e.g. 0 ; 0 ; and 0 .

The ratio $N_n/N_p = 1.00 \pm 0.05$ was found from HIJING [13] and AMPT [17] in the rapidity interval $|y| < 3.5$. The equilibration of protons and neutrons close to mid-rapidity has been experimentally observed at AGS energies [18].

At mid-rapidity the ratio $=p = 0.89 \pm 0.07$ (stat) 0.21 (syst) was found to be equal within statistical errors to $=p = 0.95 \pm 0.09$ (stat) 0.22 (syst) at $\sqrt{s_{NN}} = 130$ GeV [19]. Those results indicate that $=p = =p = N = N_p$. We use $N = N_p = 0.93 \pm 0.11$ (stat) 0.25 (syst) at $\sqrt{s_{NN}} = 200$ GeV and find at $y = 0$ the number of feed-down corrected protons and anti-protons to be $dN/dy = 17.5 \pm 1.2$ (stat) 3.0 (syst) and $dN/dy = 13.2 \pm 0.9$ (stat) 2.3 (syst) respectively, in agreement with the measurement at $\sqrt{s_{NN}} = 200$ GeV by PHENIX : $dN/dy(p) = 18.4 \pm 2.6$ (syst); $dN/dy(p) = 13.5 \pm 1.8$ (syst) [20].

At forward rapidity have not been measured, but N_{B-B} depends very weakly on N because the term in front of N in Eq. 2 is close to 0 since $c = 0.5$ and $\frac{N_n}{N_p} = 1$. Even assuming $N = N_p = 1.0 \pm 0.5$ (50% error) it is found that $N_{B-B} = 1.96 \pm 0.07$ N_p and the error on $N = N_p$ gives the smallest contribution to this error.

Figure 4 (insert) shows the net-baryon dN/dy obtained from the measured net-proton dN/dy . The net-baryon density has been fitted with two different functions with fixed integrals equal to N_{part} . The first function is a symmetric 6th degree polynomial (pol6) fit $f(y)$ with $f(y_p) = 0$. The second fit function (momgaus) is a symmetric sum of 2 Gaussians in momentum space, converted to rapidity space using $p = m \sinh(y)$ ($p_T = 0$) where m is the proton mass. From the Gaussian fit a mean momentum of 33 GeV/c with a spread of 14 GeV/c is found. The fits are all consistent with Bjorken's picture of the collision where the fragmentation regions are far from mid-rapidity ($y = 3-4$), but shows that there is still a significant number of baryons transported to mid-rapidity. The rapidity loss is $h_{yi} = 2.0 \pm 0.1$ using the pol6 fit and $h_{yi} = 2.0 \pm 0.2$ for the momgaus fit, as shown in Fig. 4. This rapidity loss is clearly less than the phenomenological linear rapidity scaling

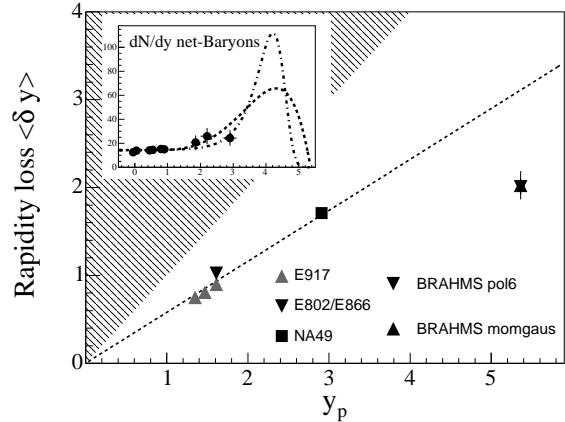


FIG. 4: The inserted plot shows the extrapolated net-baryon distribution (data points with fits represented by the curves) to the data, see text for details. The full figure shows the rapidity loss, obtained using Eq. 1, as a function of projectile rapidity (in the CM). The hatched area indicates the unphysical region and the dashed line shows the phenomenological scaling $h_{yi} = 0.58 y$. The data from lower energy are from [5, 7].

would predict; this scaling is broken at RHIC. The small increase from SPS to RHIC could be an indication that the rapidity loss saturates for such high energies.

The total energy, E , per net-baryon after the collision E can be derived:

$$E = \frac{1}{N_{part}} \int_{y_p}^{y_p} \ln_{Ti} \cosh y \frac{dN}{dy} dy \quad (3)$$

The \ln_{Ti} is known from the spectra in the covered rapidity interval. Linear and Gaussian extrapolations of \ln_{Ti} to projectile rapidity changes E by less than 5%. The energy is $E = 31 \pm 2$ GeV for pol6 and $E = 27 \pm 5$ GeV for the momgaus fit. Taking $E = 28 \pm 6$, $E = 72 \pm 6$ GeV of the initial 100 GeV per participant is available for excitations. For the 115-13 net-baryons in the measured interval, $3.0 < y < 3.0$, the energy loss is $E = 95 \pm 1$ GeV.

In conclusion BRAHMS has measured proton, anti-proton, and net-proton yields from mid-rapidity ($y = 0$) to forward rapidity ($y = 3$). The net-proton distribution shows that collisions at RHIC energies are quite transparent compared to lower energies. By extrapolation to the full net-baryon distribution, we find that the rapidity loss scaling observed at lower energy is broken and the rapidity loss seems to saturate between SPS and RHIC energies.

This work was supported by the division of Nuclear Physics of the Office of Science of the U.S. DOE, the Danish Natural Science Research Council, the Research Council of Norway, the Polish State Com. for

Scientific Research and the Romanian Ministry of Research.

- [1] S.A. Bass et al., Nucl. Phys. A 661 (1999) 205.
- [2] S. So, J. R andrup, H. Stocker and N. Xu, Phys. Lett. B 551 (2003) 115.
- [3] S. A. Bass, B. M uller and D. K. Srivastava, Phys. Rev. Lett. 91 (2003) 052302.
- [4] W. Busza and A. S. Goldhaber, Phys. Lett. B 139 (1984) 235.
- [5] F. V. Videbaek and O. Hansen, Phys. Rev. C 52 (1995) 2684.
- [6] B. Hong et al. [FOPI Collaboration], Phys. Rev. C 57 (1998) 244 [Phys. Rev. C 58 (1998) 603].
- [7] B. B. Back et al. [E917 Collaboration], Phys. Rev. Lett. 86 (2001) 1970.
- [8] J. D. B jorken, Phys. Rev. D 27 (1983) 140.
- [9] F. Karsch, Nucl. Phys. A 698 (2002) 199.
- [10] M. Adamczyk et al. [BRAHMS Collaboration], Nucl. Instr. and Meth. A 499 (2003) 437.
- [11] I. G. Bearden et al. [BRAHMS Collaboration], Phys. Rev. Lett. 88 (2002) 202301.
- [12] GEANT 3.2.1, CERN program library.
- [13] X. N. Wang and M. Gyulassy, Phys. Rev. D 44 (1991) 3501.
- [14] L. Ahle et al. [E802 Collaboration], Phys. Rev. C 60 (1999) 064901.
- [15] J. Barette et al. [E877 Collaboration], Phys. Rev. C 62 (2000) 024901.
- [16] H. Appelshauser et al. [NA49 Collaboration], Phys. Rev. Lett. 82 (1999) 2471.
- [17] B. Zhang, C. M. Ko, B. A. Li and Z. w. Lin, Phys. Rev. C 61 (2000) 067901.
- [18] K. N. Barish et al., Phys. Rev. C 65 (2002) 014904.
- [19] K. Adcox et al. [PHENIX Collaboration], Phys. Rev. Lett. 89 (2002) 092302.
- [20] S. S. Adler et al. [PHENIX Collaboration], Subm itted to Phys. Rev. C, arX iv:nucl-ex/0307022.
- [21] The rapidity is defined as $y = 0.5 \ln \frac{E + p_z}{E - p_z}$ and in the rest of the text a coordinate system where y_p is positive and mid(rapidity $y_m = 0$, is used, i.e., the CM system for symmetric collisions.